ORNL/TM-8179
Dist. Category UC-20 a,f

Contract No. W-7405-eng-26

ORNL/TM--8179

DE82 015818

FUSION ENERGY DIVISION

HARD X-RAY MEASUREMENTS OF THE HOT-ELECTRON RINGS IN EBT-S

D. L. Hillis

NOTICE This document contains information of a preliminary nature. *It is subject to revision or correction and therefore does not represent a* final report.

Date Published - June 1982

Prepared by the
OAK RIDGE NATIONAL LABORATORY
Oak Ridge, Tennessee 37830
operated by
UNION CARBIDE CORPORATION
for the
DEPARTMENT OF ENERGY

CONTENTS

ABSTRACT

A thorough understanding of the hot electron rings in ELMO Bumpy Torus-Scale (EBT-S) is essential to the bumpy torus concept of plasma production, since the rings provide bulk plasma stability. The hot electrons are produced via electron cyclotron resonant heating using a 28-GHz cw gyrotron, which has operated up to power levels of 200 kW. The parameters of the energetic electron rings are studied via hard x-ray measurement techniques and with diamagnetic "pickup" coils. The hard x-ray measurements have used collimated NaI(Tl) detectors to determine the electron temperature T_e and electron density n_e for the hot electron annulus. Typical values of T_e are 400-500 keV and of n_e 2-5 $\times$ 10^{11} cm^{-3}. The total stored energy of a single energetic electron ring as measured by diamagnetic pickup loops approaches $\sim$40 J and is in good agreement with that deduced from hard x-ray measurements. By combining the experimental measurements from hard x-rays and the diamagnetic loops, an estimate can be obtained for the volume of a single hot electron ring. The ring volume is determined to be $\sim$2.2 litres, and this volume remains approximately constant over the T-mode operating regime. Finally, the power in the electrons scattered out of the ring is measured indirectly by measuring the x-ray radiation produced when those electrons strike the chamber walls. The variation of this radiation with increasing microwave power levels is found to be consistent with classical scattering estimates.

1. INTRODUCTION

An essential feature of the ELMO Bumpy Torus (EBT)[1,2] is the presence of an energetic electron annulus in each of the 24 mirror sectors. These high-beta ($\beta \sim 25\%$) annuli are formed and sustained solely by steady-state microwaves resonant at the electron cyclotron frequency. The presence of the hot electron annulus[3,4] modifies the unfavorable vacuum field and acts to stabilize the toroidally confined core plasma against interchange modes.

The magnetic field configuration in EBT-I ($B_{res} \cong 0.64$ T) utilizes klystrons that deliver up to 60 kW for primary electron cyclotron resonance heating (ECRH) near the mirror throats and 30 kW of 10.6-GHz microwave power mainly for profile heating near the outer radial boundary of the plasma. Recently, additional ECRH was added to EBT using a 28-GHz cw gyrotron that was operated at power levels of up to 200 kW. This upgraded EBT, which distributes the 200 kW of 28-GHz microwave power and provides the higher resonant magnetic field ($B_{res} \cong 1$ T), is called EBT-S. Typical machine characteristics and physical dimensions for EBT can be found in Refs. 1 and 2.

The overall behavior of the EBT toroidal streaming plasma is dependent upon the microwave power P_μ and the background neutral pressure p_o. (1) The C-mode occurs at high ambient pressure and/or low microwave power and is characterized by a cold, dense, and noisy plasma. No energetic electrons are present. (2) The T-mode occurs at lower pressure when hot electron rings form and produce a quiescent toroidally streaming plasma that is macrostable. Electron temperatures approaching 1 keV have been observed for this toroidally streaming bulk plasma during T-mode operation with 200 kW of 28-GHz microwave power. (3) Finally, the M-mode occurs at still lower pressures, the plasma begins to exhibit instabilities, and the torus begins to appear as disconnected mirror segments.

The purpose of this paper is to investigate the properties of the hot electron rings of EBT-S. The x-ray energy distribution of free-free bremsstrahlung (continuum radiation) in the hard x-ray regime has been

measured to determine the electron temperature T_e and density n_e of the hot electron annuli of EBT-S. The x-ray analysis system utilizes a calibrated NaI(Tl) detector for these measurements. First, the experimental results are presented for EBT-S as a function of the controllable parameters microwave power P_μ and ambient pressure p_o. The first results on ring parameters from EBT-S when operated at cw microwave powers of up to 200 kW at 28 GHz are reported herein. Hard x-ray results indicate that the energetic electron rings have electron temperatures of $\sim$450 keV and that densities of about 3.0×10^{11} cm^{-3} are obtainable. Additional information is obtained about the ring stored energy from diamagnetic pickup loops. Finally, our conclusions about the properties of hot electron rings on EBT-S are presented.

2. EXPERIMENTAL DETAILS

The x-ray energy distribution of free-free bremsstrahlung in the hard x-ray regime (50 keV-2.5 MeV) is measured with a calibrated (12.7 cm $\times$ 12.7 cm) NaI(Tl) detector. The hard x-ray detection system used on EBT-S is shown in Fig. 1. The NaI detector is collimated to view a single chord in the midplane region of a single EBT-S cavity. The energetic electron ring is located midway between two of the toroidal field coils, has a radius of 12.5 cm as measured from the plasma center and is located at the second harmonic resonance of the applied microwave frequency. Incoming x-rays that strike the NaI detector produce voltage pulses whose pulse height is proportional to the photon energy E. The resultant pulses are sorted according to their energies and counted by a Nuclear Data ND6600 computer based pulse height analysis system to yield an x-ray energy spectrum. A series of Pb collimators is used to ensure that the detector sees only a small, well-defined single chord of the ring plasma. To reduce the hard x-ray attenuation (due to the thick aluminum vacuum vessel of EBT), a thin aluminum x-ray window of 0.025 cm is used along the detector line of sight. The NaI detector's energy calibration, as well as its detection efficiency, was obtained by using a set of nine calibrated gamma ray sources.

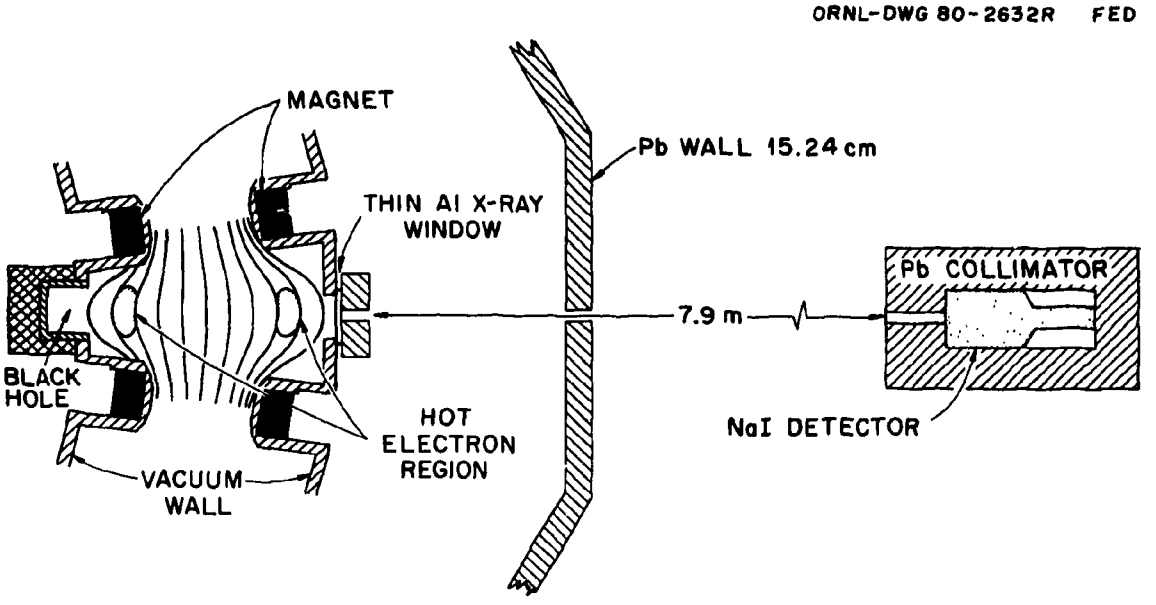

Fig. 1. The NaI detection system used on EBT for hard x-ray measurements.

Figure 2(a) shows a typical hard x-ray spectrum obtained for an EBT-S plasma with an applied microwave power P_μ = 50 kW at 28 GHz and a filling pressure of 6.0×10^{-6} torr. The spectrum has been corrected for detector efficiency, attenuation of x-rays due to air, and the thin aluminum x-ray window. The most notable feature of the spectrum of Fig. 2(a) is its lack of structure. The hard x-ray energy distribution arising from the rings appears to be a continuum of radiation that can be represented by a single exponential.

The x-ray bremsstrahlung from a hydrogenic plasma has been treated extensively in the literature.[5-7] For a Maxwellian plasma the free-free bremsstrahlung emission is given by

$$\frac{dW}{dE} = 3.2 \times 10^{-15}\, n_e \ell n_i Z_i^2 T_e^{-1/2} g_{ff} \exp^{(-E/T_e)}\, A\, \frac{\Omega}{4\pi}\,, \qquad (1)$$

where dW is the radiated power per second into the photon energy interval dE, n_e and n_i are the electron and ion density, respectively, Z_i is the ion charge of the scattering center, g_{ff} is the temperature average gaunt factor, T_e is the electron temperature, E is the x-ray photon energy, A is the plasma area viewed by the NaI detector whose solid angle is Ω, and ℓ is the effective chord length of plasma seen by the detector. For typical operating regimes present on EBT-S we are justified in assuming that (1) all electron scattering is due to hydrogen ions ($Z_i^2 \approx 1$) and (2) the energetic electrons of the rings scatter from the bulk ion population n_i, which exists at the ring location. The electron temperature can then be extracted from the measured photon energy distribution by calculating the inverse slope of the data in a semilogarithmic plot of intensity dW/dE versus x-ray energy. The line averaged electron density $n_e\ell$ can also be found by evaluating Eq. (1) after T_e is determined.

The determination of n_i is taken from an independant measurement of the electron density for the bulk plasma using a multichord microwave interferometer. The bulk plasma electron density at the ring location is assumed to be equal to n_i.

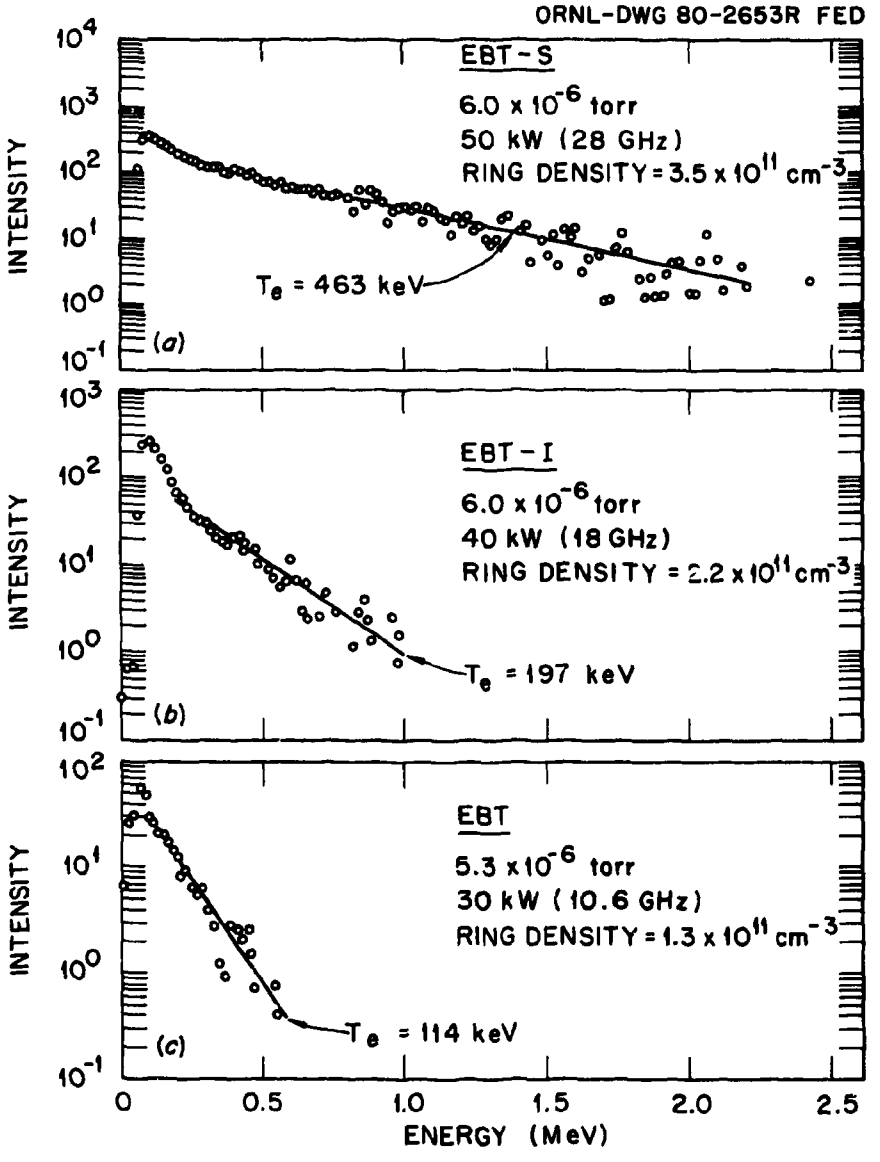

Fig. 2. Typical hard x-ray bremsstrahlung spectra observed during EBT operation when single-frequency microwave heating was used to form the energetic electron rings; (a), (b), and (c) show x-ray spectra generated when 28-, 18-, and 10.6-GHz microwave heating frequencies, respectively, were used. The spectra were obtained with a calibrated NaI detector.

3. EXPERIMENTAL RESULTS

Shown in Fig. 2 are three typical spectra obtained for EBT plasmas under three different operating conditions. Three separate microwave systems of 10.6, 18, and 28 GHz are available on EBT. Steady-state klystrons deliver up to 30 kW of 10.6-GHz microwaves and up to 60 kW of 18-GHz microwaves on EBT. The most recent addition to EBT is a cw gyrotron that delivers up to 200 kW of 28-GHz microwaves. Each of the three hard x-ray spectra shown in Fig. 2 corresponds to single-frequency ECRH. The magnetic field on EBT is adjusted for each microwave frequency such that the energetic electron rings are produced at the second harmonic of the electron cyclotron frequency and at the same location within the EBT cavity.

The three spectra, shown in Figs. 2(a)-2(c), are clearly quite different. By utilizing the techniques outlined in Section 2, the electron temperature T_e and density n_e are determined from a least-squares fit to the experimental data. Clearly, both the ring temperature and ring density increase with microwave frequency. Ring temperatures of $\sim$450 keV were obtained for the 28-GHz microwave frequency.

Following the general analysis procedure outlined in Section 2, T_e and n_e for the hot electron rings were measured for a variety of different operating conditions on EBT-S. Both the applied microwave power out of the 28-GHz gyrotron P_μ and the ambient gas pressure ρ_o were varied with hard x-ray spectra being measured at each new condition. To illustrate the microwave power dependence of T_e and $n_e\ell$, Figs. 3 and 4 show T_e and $n_e\ell$ plotted as functions of P_μ at constant pressure. The values of T_e do not have a strong variation with either microwave power or ambient pressure. The values of $n_e\ell$, however, do vary appreciably with both P_μ and ρ_o, with the highest densities being achieved at the highest values of P_μ or the lowest values of ρ_o. The thickness of the hot electron ring has been measured using a skimmer probe and found to be 2.5 cm. The hard x-ray measurement sees an effective chord length of 5.0 cm and therefore indicates that the ring densities n_e are $\sim 4.2 \times 10^{11}$ cm^{-3} at the highest ECRH power levels. The three pressures are chosen to span most of the T-mode operating regime, where rings are

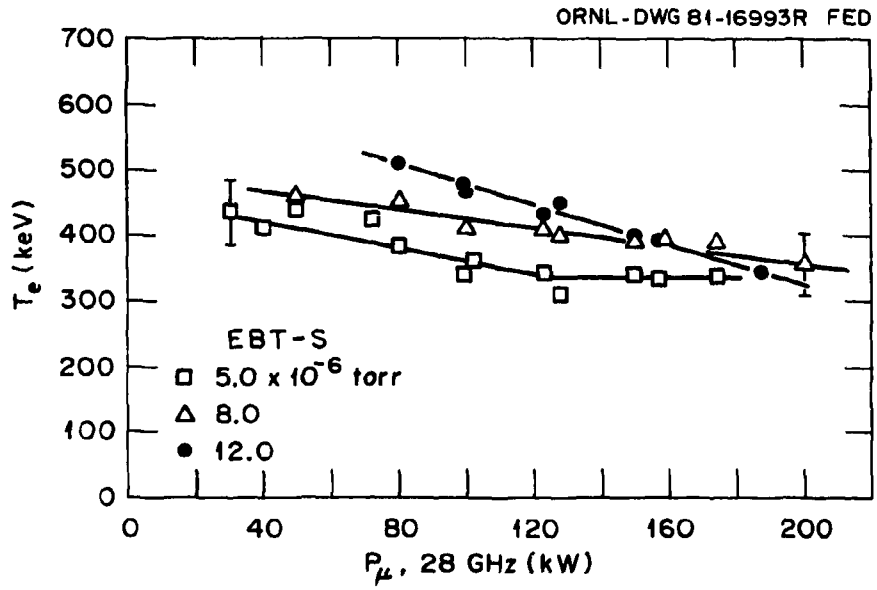

Fig. 3. The electron temperature, as measured by the hard x-ray detection system, is plotted against microwave power out of the 28-GHz gyrotron for several values of ambient pressure (5×10^{-6}, 8×10^{-6}, and 12×10^{-6} torr).

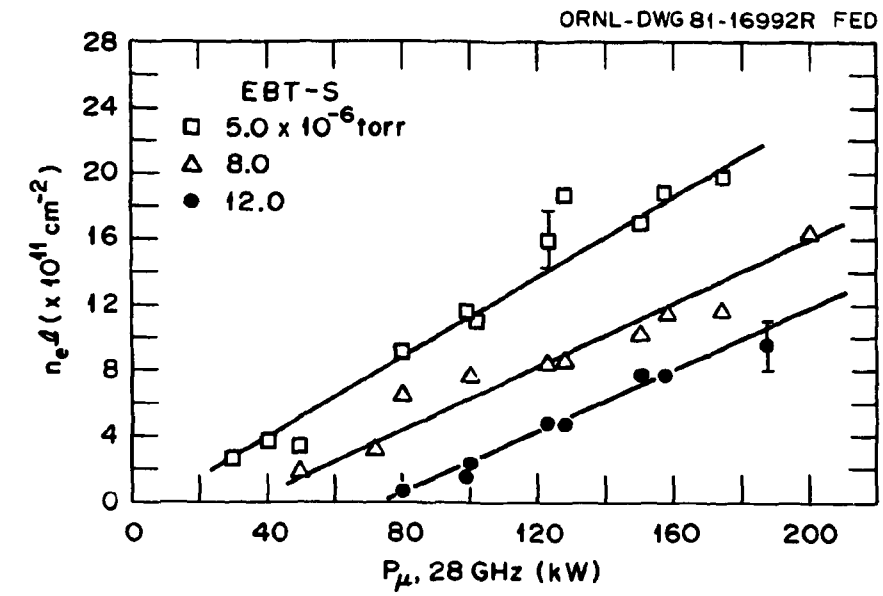

Fig. 4. The line averaged electron density $n_e \ell$, as measured by the hard x-ray detection system, is plotted against microwave power out of the 28-GHz gyrotron for several values of ambient pressure (5×10^{-6}, 8×10^{-6}, and 12×10^{-6} torr).

present. Even though a slight decrease in T_e for the ring is observed with increasing P_μ, the ring temperature does not change markedly from its average value of $T_e \approx 450$ keV. Figure 4 shows that the major change in the ring occurs in $n_e\ell$, where the ring density is observed to increase with increased microwave power and/or neutral pressure.

As was pointed out earlier, EBT has three microwave frequencies (10.6, 18, and 28 GHz) with which to form the energetic electron rings. The magnetic field is varied such that the hot electron rings are formed at the second harmonic resonance of the applied ECRH and at the same radial location within the EBT cavity. The same variations of T_e and $n_e\ell$ with respect to P_μ and ρ_o are observed with the 18- and 10.6-GHz microwave sources, as shown in Figs. 3 and 4. However, major changes in the absolute values of T_e and n_e do occur with the applied microwave frequency. Figure 5 shows the range of values for T_e and n_e observed for the rings when the rings are heated via single-frequency microwaves. The various data points shown at each microwave frequency are points acquired over a range of different values of P_μ and ρ_o where the rings are present. Even though T_e varies only slightly with P_μ and ρ_o for 28-GHz microwave heating (see Fig. 3), dramatic changes in T_e occur as the microwave heating frequency is varied. This is also indicated in the three hard x-ray spectra shown in Fig. 2. The values of both T_e and n_e are shown in Fig. 5 to increase dramatically with the applied microwave frequency. It should be noted that the frequency axis could equally well be replaced by the magnetic field at the ring location that is needed to produce the necessary electron resonance at the second harmonic of the applied microwave frequency.

As a separate ring diagnostic, each of the EBT cavities is surrounded by diamagnetic pickup loops. By measuring the induced currents in these pickup coils due to the energetic electron rings, the stored energy can be determined for an individual electron ring. Figure 6 shows the stored energy of a single EBT-S ring as deduced from these diamagnetic loops as a function of ρ_o at a variety of values of P_μ. At the lowest pressures and highest P_μ, rings are produced with up to 40 J of stored energy.

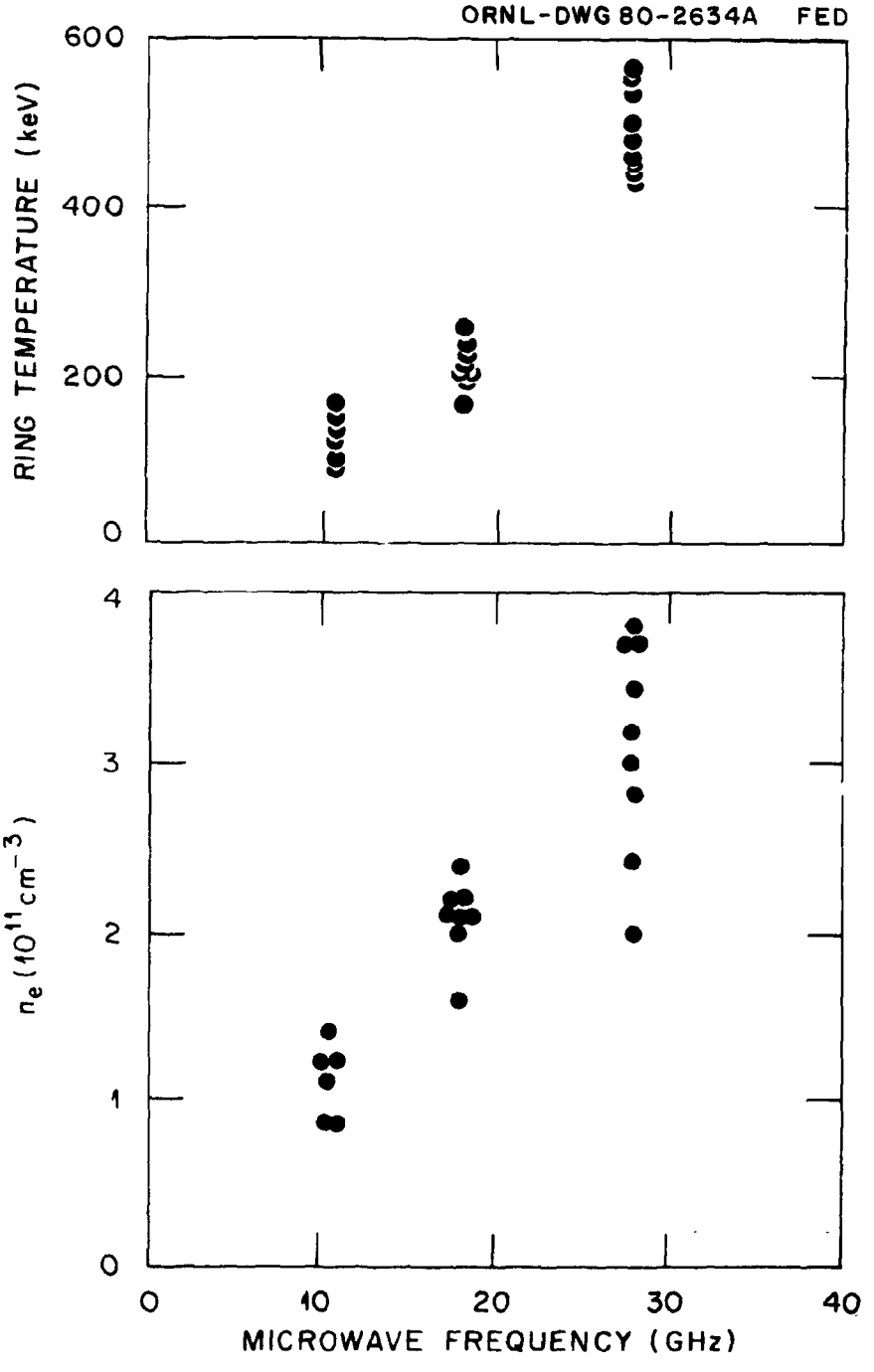

Fig. 5. Ring temperature and ring density variations with the applied microwave frequency. The range of data points at each frequency corresponds to a wide range of experimental conditions for P_μ and ρ_o.

4. PROPERTIES OF THE HOT ELECTRON RINGS

The rings of EBT must form with sufficient stored energy $W_\perp$ to modify the magnetic field gradients and to provide an average minimum-B stabilization of the toroidally streaming core plasma. Experimentally, stabilization of the core plasma is characterized by a reduction in density fluctuations and by the formation of a symmetric ambipolar potential well.[8] This is known as the C-T transition region and is the point at which the ring just forms. Experimentally, the ring stored energy at the C-T transition is just a few joules and is approximately constant for large changes in microwave power and pressure. This is illustrated by the crosshatched region of Fig. 6.

At the lowest pressure and the very highest ring stored energies at each value of P_μ, another operating boundary is encountered — i.e., the T-M transition. This is also shown in Fig. 6. At the T-M transition the EBT rings begin to exhibit instabilities and finally disappear at still lower pressures. The region of interest for normal EBT operation is the T-mode regime, as this is the region where all of the basic EBT concepts are at work. Another important feature shown in Fig. 6 is the wider operating regime (pressure window) for the T-mode, which occurs at the higher values of P_μ.

From the hard x-ray measurements of the ring T_e and n_e, the average ring beta β can be calculated according to

$$\beta = \frac{8\pi n_e T_e}{B_r^2} , \qquad (2)$$

where B_r is the magnetic field at the ring location (B_r = 0.5 T for EBT-S). The values for both n_e and T_e are the result of chord integrated measurements and therefore represent average values for these parameters. Figure 7 shows ring beta plotted as a function of microwave power for constant ambient gas pressures. Ring betas approaching 25% are obtained for the highest values of applied microwave power. It is encouraging that ring beta, as well as ring stored energy, continues to increase as the applied microwave power is increased.

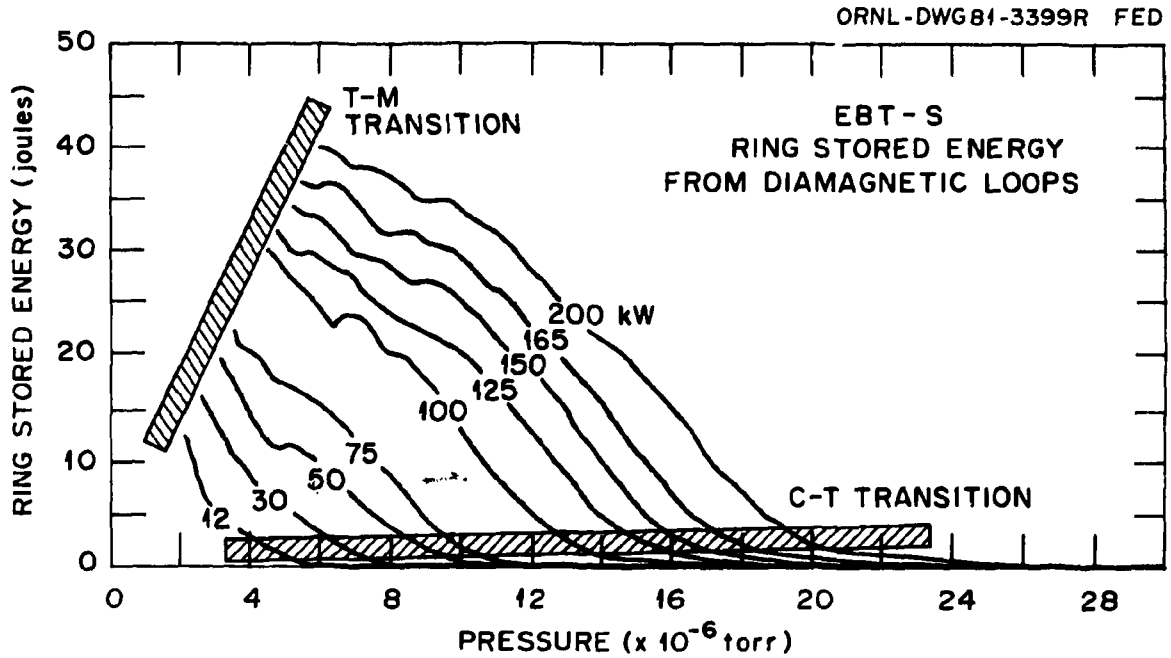

Fig. 6. Experimental measurements of the stored energy of a single EBT-S hot electron ring as a function of operating pressure for various amounts of applied 28-GHz microwave power. The locations of the C-T and T-M operating boundaries are indicated by the crosshatched regions.

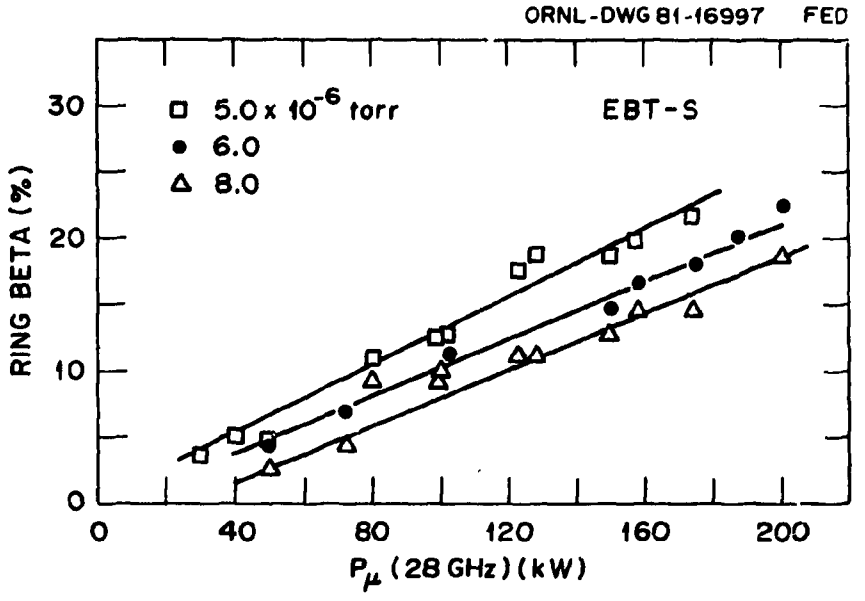

Fig. 7. The hot electron ring beta is plotted as a function of applied 28-GHz microwave power for several values of ambient pressure (5×10^{-6}, 8×10^{-6}, and 12×10^{-6} torr). The ring beta is deduced from the hard x-ray measurements of T_e and n_e.

By combining the information obtained from the rings by the hard x-ray diagnostic and the diamagnetic loops, information can be obtained about the volume of the hot electron ring plasma. The energy density of the hot electron ring is obtained from the hard x-ray measurements of T_e and n_e, since

$$\text{energy density} = \frac{W_\perp}{V_A} = n_e T_e \ , \tag{3}$$

where V_A is the ring plasma volume. The diamagnetic loop diagnostic, however, measures the ring stored energy $W_\perp$ directly. By plotting $W_\perp$ (diamagnetic loop)/$n_e T_e$ (hard x-ray) versus $W_\perp$ from the diamagnetic loops, the volume of the hot electron ring can be determined as a function of stored energy. This is shown in Fig. 8 for a variety of microwave power levels and ambient pressures. Over the entire range of conditions studied the annulus volume appears to be constant at an average value of about 2.2 litres.

From skimmer probe measurements the hot electron ring is known to have a radius $a_p \sim 12.5$ cm and a thickness $\delta_A \sim 2.5$ cm. The axial extent of the ring, L_A, is less well known but can be inferred from these measurements. For simplicity we take the annulus volume to be

$$V_A = 2\pi a_p \delta_A L_A \ , \tag{4}$$

which infers an axial extent for the ring $L_A \sim 10$ cm. Since we have observed that large changes in the ring volume are not apparent over our data set, the ring dimensions are also not expected to change dramatically over the T-mode operating regime.

Another area of importance for EBT-type devices is the overall radiation level produced by the energetic electrons that are scattered out of the ring and strike the vacuum chamber wall, producing thick target bremsstrahlung. These electron scattering losses from the rings are measured indirectly by measuring the overall x-ray level (R/h) observed within the EBT lead enclosure with a calibrated Reuter-Stokes

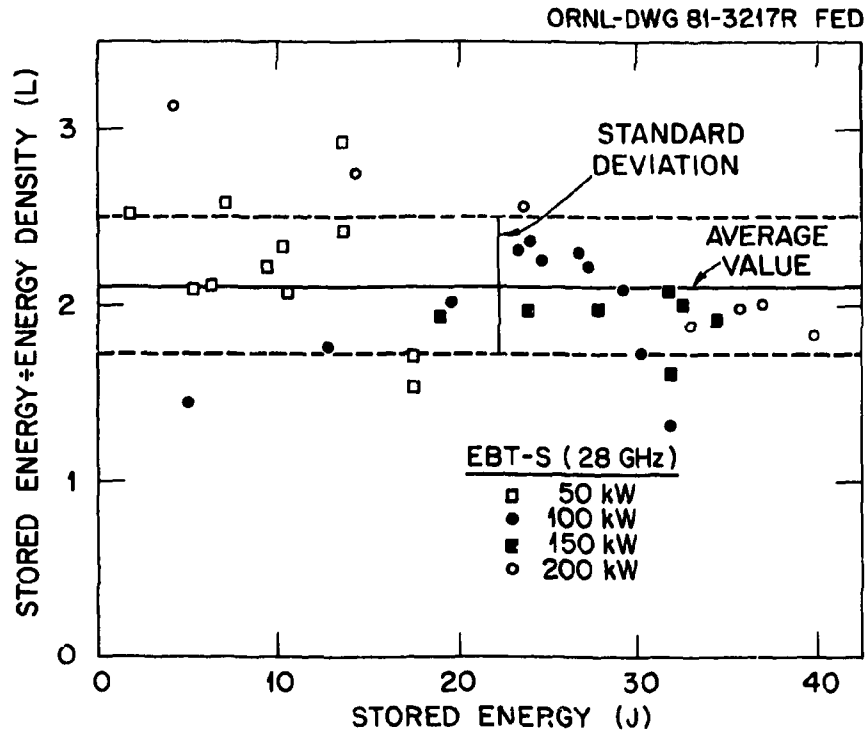

Fig. 8. The volume of a single hot electron ring for EBT-S is plotted against the ring stored energy. The various data points correspond to a variety of conditions for P_μ and ρ_o. (See text for detailed explanation.) A ring volume of ~2.2 liters is found using this experimental technique.

nitrogen-filled ionization chamber. The ionization chamber is centrally located near the center of EBT. On the basis of classical scattering the thick target bremsstrahlung observed in this detector is given by[9]

$$P_b \propto Z_W n_e n_i T_e^{1/2} V_A \ , \tag{5}$$

where P_b is the radiated power in the form of x-rays generated when energetic electrons scatter from the ring and strike the vacuum vessel wall of atomic number Z_W. Figure 9 shows the radiation level observed inside the EBT lead enclosure as the stored energy of each individual EBT ring is increased. Clearly, as more energetic rings are produced in EBT at the higher microwave powers, the radiation level becomes greater within the lead enclosure. With 200 kW of ECRH power more than 3000 R/h is produced within the enclosure.

Utilizing the relation of Eq. (5), the enclosure radiation is plotted against $n_e n_i T_e^{1/2}$ in Fig. 10. The values of n_e and T_e are determined from our hard x-ray measurements, whereas n_i is determined from microwave interferometer results described earlier herein. Figure 10 illustrates that the variation of the enclosure radiation is consistent with classical scattering.

High-beta, hot electron plasmas have been produced with ECRH in several experiments other than EBT. Details of these experiments can be found in Ref. 4. A wide variety of conditions was present in these experiments, where (a) magnetic fields varied from 1 to 10 kg, (b) microwave heating frequencies varied from 6 to 55 GHz, and (c) hot electrons were produced with temperatures from 50 to 1200 keV. An analysis of these other ECRH experiments[8] is shown in Fig. 11, where the temperature of the hot electron annulus is plotted for each experiment as a function of the resonance magnetic field at the ring location. These data are all for single-frequency ECRH and indicate that the hot electron temperatures increase with magnetic field strength or equivalently with the microwave frequency. These data are then compared with the results obtained from EBT, which were presented earlier in Fig. 5. The ring temperature, microwave frequency, and magnetic field are all important in determining the hot electron gyroradius. The solid curves show that

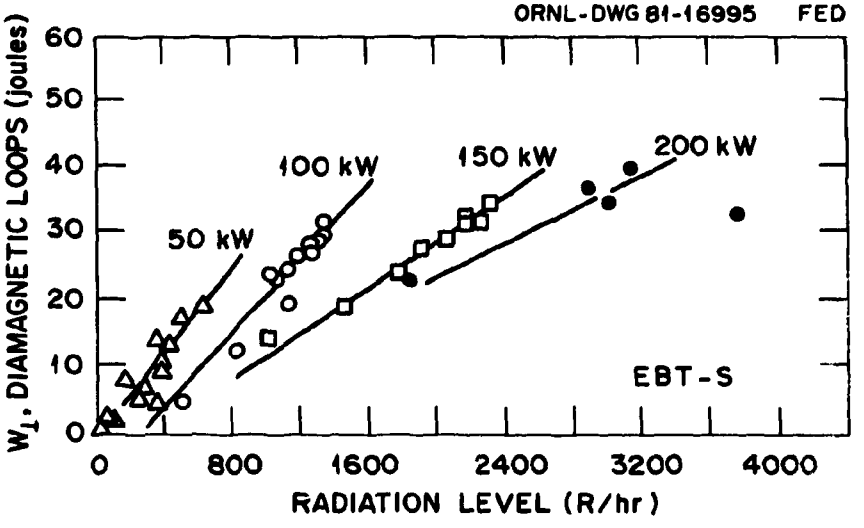

Fig. 9. The stored energy of a single hot electron ring is plotted against the overall enclosure radiation observed for EBT-S. The various data points correspond to a variety of operating conditions due to changes in P_μ and ρ_o. (See text for discussion.)

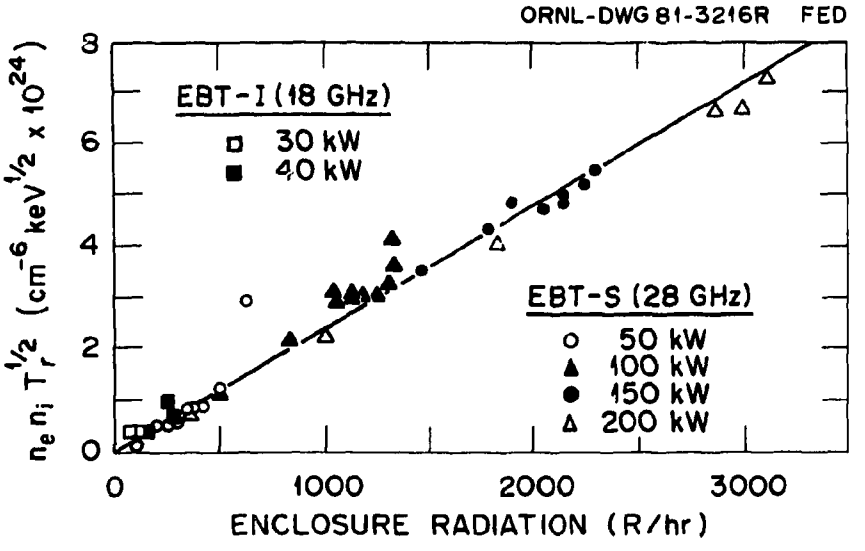

Fig. 10. The quantity $n_e n_i T_r^{1/2}$ is plotted against the enclosure radiation found for EBT-S. The various data points correspond to a variety of operating conditions due to changes in P_μ and ρ_o. This variation of the enclosure radiation is consistent with classical scattering estimates.

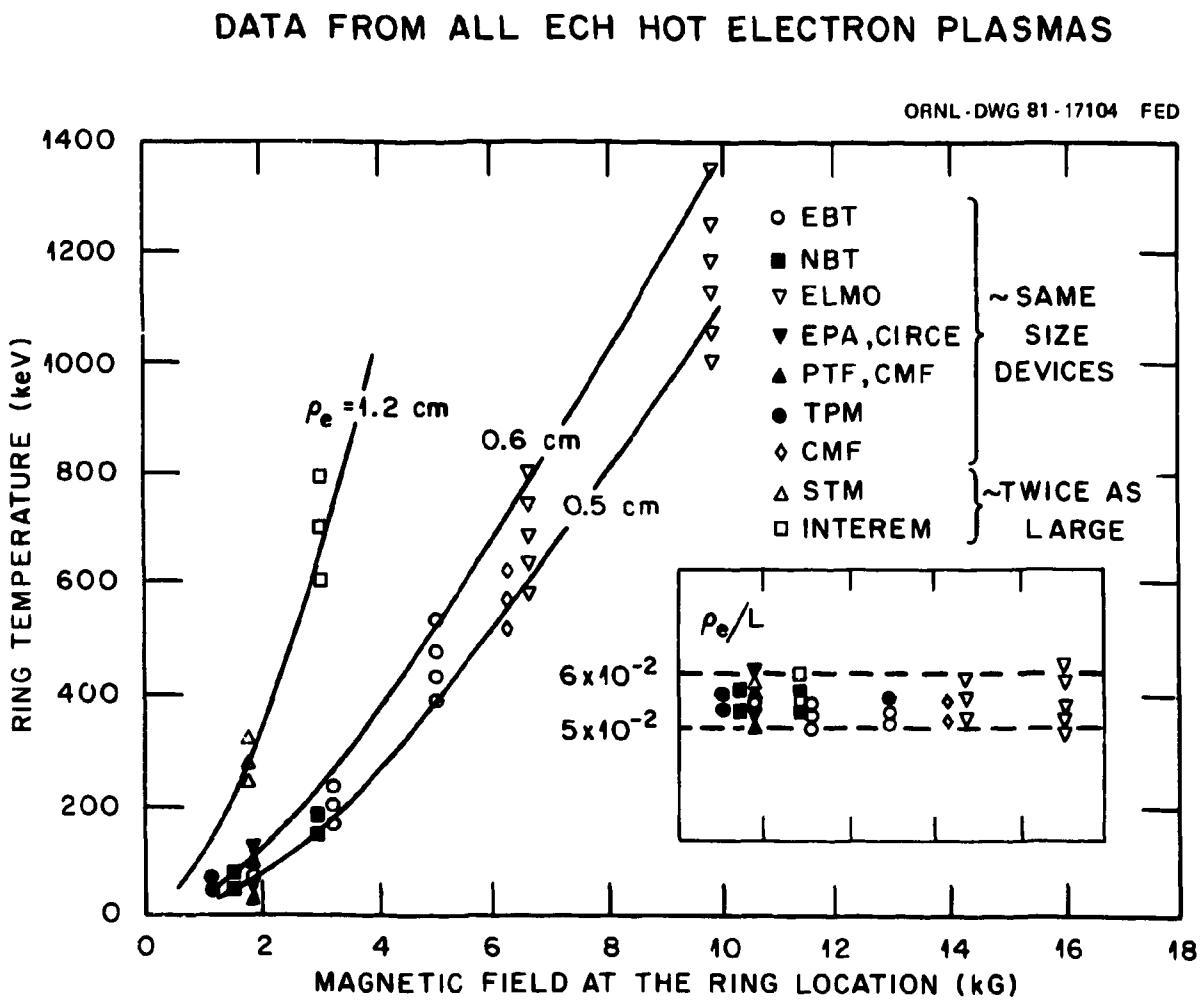

Fig. 11. Ring temperature is plotted as a function of magnetic field at the ring location for a variety of microwave heated hot electron plasmas. The data are compared to the EBT-S results. The solid lines are for constant hot electron gyroradii ρ_e, as shown. Data from all of the above hot electron plasmas can be represented by a value of $\rho_e/L \approx 0.05\text{-}0.06$, where L is a magnetic field scale length (see insert). Data from all of these hot electron plasmas indicate that the ring temperatures obey a simple ρ_e/L scaling.

the data from the various ECH experiments, as well as EBT, can be understood on the basis of a constant relativistic gyroradius ρ_e between 0.5 and 0.6 cm. The data from the STM and Interem devices, however, require a larger ρ_e of 1.2 cm. These two devices are much larger in physical dimensions than the other devices. By using an appropriate magnetic scale length L for each device, the values of ρ_e/L are displayed within the insert of Fig. 11. For all of the devices investigated, the dimensionless constant ρ_e/L appears to be a constant and lies between 0.05 and 0.06.[8] The observation that $\rho_e/L \approx$ constant on the devices discussed herein may be an important quantity to be addressed on newly proposed ECRH devices.

REFERENCES

1. R. A. Dandl et al., ORNL/TM-3694 (1971); R. A. Dandl et al., Plasma Physics and Controlled Nuclear Fusion Research 1974, Vol. II, 141 (1975).
2. J. C. Glowienka, J. Vac. Sci. Technol. 18(3), 1088 (1981).
3. R. A. Dandl et al., Plasma Physics and Controlled Nuclear Fusion Research 1968, Vol. II, 435 (1975); R. A. Dandl et al., Plasma Physics and Controlled Nuclear Fusion Research 1971, Vol. II, 607 (1972).
4. N. A. Uckan, ed., EBT Ring Physics: Proceedings of Workshop, Conf.-791228, Oak Ridge, Tennessee (1979).
5. T. F. Stratton, Plasma Diagnostic Techniques (Academic Press, New York, 1965) 362.
6. S. von Goeler, Diagnostics for Fusion Experiments, edited by E. Sindoni and C. Wharton (Pergamon Press, Oxford and New York, 1979) 79.
7. R. J. Gould, Astrophys. J. 238, 1026 (1980).
8. N. A. Uckan, ORNL/TM-8006 (1981) and Proceedings of 10th European Conference on Controlled Fusion and Plasma Physics (to be published).
9. H. Knoepfel, Diagnostics for Fusion Experiments, edited by E. Sindoni and C. Wharton (Pergamon Press, Oxford and New York, 1979) 111.